

MASS TRANSFER, TRANSITING STREAM, AND MAGNETOPAUSE IN CLOSE-IN EXOPLANETARY SYSTEMS WITH APPLICATIONS TO WASP-12

DONG LAI^{1,4}, CH. HELLING^{2,4}, AND E.P.J. VAN DEN HEUVEL^{3,4}

Draft version November 18, 2018

ABSTRACT

We study mass transfer by Roche lobe overflow in close-in exoplanetary systems. The planet’s atmospheric gas passes through the inner Lagrangian point and flows along a narrow stream, accelerating to 100-200 km s⁻¹ velocity before forming an accretion disk. We show that the cylinder-shaped accretion stream can have an area (projected in the plane of the sky) comparable to that of the planet and a significant optical depth to spectral line absorption. Such a “transiting cylinder” may produce an earlier ingress of the planet transit, as suggested by recent HST observations of the WASP-12 system. The asymmetric disk produced by the accretion stream may also lead to time-dependent obscuration of the starlight and apparent earlier ingress. We also consider the interaction of the stellar wind with the planetary magnetosphere. Since the wind speed is subsonic/sub-Alfvénic and comparable to the orbital velocity of the planet, the head of the magnetopause lies eastward relative to the substellar line (the line joining the planet and the star). The gas around the magnetopause may, if sufficiently compressed, give rise to asymmetric ingress/egress during the planet transit, although more works are needed to evaluate this possibility.

Subject headings: hydrodynamics - planetary systems - stars: individual (WASP-12) - stars: winds, outflows

1. INTRODUCTION

The close-in exoplanets (with period less than a few days) discovered in radial velocity and transit surveys are of great interest, not only because they constrain theories of planet formation and evolution, but also because they provide a probe of various physical processes that are otherwise unimportant in “normal” planets. WASP-12b is a transiting exoplanet orbiting extremely close to a late-F/early-G star ($M_\star = 1.35M_\odot$, $R_\star = 1.57R_\odot$, $T_{\text{eff}} = 6300$ K), with the orbital period $P = 1.09$ days and orbital semi-major axis $a = 0.023$ AU = $4.94R_\odot = 3.15R_\star$. The planet mass $M_p = 1.41M_J$ and radius $R_p = 1.79R_J$, as determined by transit observation in optical continuum (Hebb et al. 2009; Campo et al. 2010). The planet is one of the most irradiated exoplanets (with equilibrium temperature $T_{\text{eq}} = 2500$ -3000 K) and is highly inflated. The fact that the Roche radius (Hill sphere radius) of the planet, $R_L = a(M_p/3M_\star)^{1/3} = 1.85R_p$, is only slightly larger than the R_p derived from optical transit measurements, suggests that mass loss from the planet is likely (Li et al. 2010). The small orbital separation also suggests that stellar wind may influence the atmosphere the planet.

Recently, Fossati et al. (2010) obtained near-UV transmission spectroscopy of WASP-12b with the Cosmic Origins Spectrograph on the *Hubble Space Telescope*. The data revealed enhanced transit depths (by about a factor of 2) in two wavelength bands, NUVA (2539-2580 Å) and

NUVC (2770-2811 Å), which were attributed to flux attenuation by absorption lines of metals in the vicinity of the planet. Most interestingly, the NUVA data exhibits an earlier ingress compared to the transit in optical J,B and Z bands, while the egress of the transit occurs at about the same time as the optical transit.

The asymmetric behavior of the ingress/egress in the NUVA band relative to the continuum is difficult to understand if the absorbing gas surrounding the planet arises entirely from an irradiation-driven wind – such a wind has been studied extensively in the context of hot Jupiter HD 209458b (e.g., Yelle 2004; Tian et al. 2005; Garcia Munoz 2007; Murray-Clay et al. 2009): The wind is most strongly generated at the planet’s dayside, and would be distributed on both sides (terminations) of the substellar line (the line joining the planet and the star). If anything, it would be preferentially on the west side because of the planetary rotation, which is almost likely synchronized with the orbit (see Schneider et al. 2007 for a simulation).

In this paper, we consider two possible explanations for the asymmetric excess absorption during WASP-12b transit. First, we study the Roche lobe overflow from the planet to the parent star (see Li et al. 2010) and the associated accretion stream. The stream is asymmetric with respect to the line joining the planet and the star. We show that the stream has a sky-projected area comparable to the projected planet area, and a sufficiently large column density to cause blockage of the star light prior to optical ingress. Second, we qualitatively discuss the magnetopause produced by the interaction between the stellar wind and the planet’s magnetosphere. Because the planet’s orbital velocity, $v_{\text{orb}} = (GM_\star/a)^{1/2} = 228$ km s⁻¹, is comparable to the stellar wind velocity ($v_w \simeq 100$ km s⁻¹ at $a = 0.023$ AU), the head of the magnetopause lies eastward relative to the substellar point.

¹ Department of Astronomy, Cornell University, Ithaca, NY 14853, USA. Email: dong@astro.cornell.edu

² SUPA, School of Physics and Astronomy, University of St Andrews, North Haugh, St Andrews, KY16 9SS, UK

³ Astronomical Institute “Anton Pannekoek” and Center for High Energy Astrophysics, University of Amsterdam, The Netherlands

⁴ KITP, University of California, Santa Barbara, CA 93106

Again, ingress/egress asymmetry may be produced if the gas density in around the magnetopause is sufficiently high.

This paper is organized as follows. In Sect. 2 we discuss line absorption by a moving medium with a velocity gradient and derive the observational constraints on the absorbing gas in WASP-12b. In Sect. 3 we study the property of the accretion stream and the obscuration of the star light by the stream. Section 4 examines the possibility that the gas around the magnetopause may absorb the star light. We conclude in Sect. 5.

2. OBSERVATIONAL CONSTRAINT ON THE EXCESS ABSORBING GAS

We first consider line absorption of stellar radiation by the gas around the planet and beyond (e.g., in the accretion stream). The absorbing gas has a finite temperature T and line-of-sight bulk velocity V_{\parallel} , both of which (in general) depend on the spatial position \mathbf{r} . We denote the velocity distribution of the column density of the gas (of a given species i) by

$$\frac{dN_i}{dV_{\parallel}} = \int dl \frac{dn_i(V_{\parallel}, l)}{dV_{\parallel}}, \quad (1)$$

where the integration is along the line of sight, and dn_i/dV_{\parallel} is the velocity distribution of the gas density. The stellar radiation intensity $I_{\nu}^{(0)}$ is attenuated to $I_{\nu} = I_{\nu}^{(0)} \exp(-\tau_{\nu})$ after passing through the absorbing gas, with the optical depth given by

$$\tau_{\nu} = \int \sigma_{\nu}(V_{\parallel}) \frac{dN_i}{dV_{\parallel}} dV_{\parallel}. \quad (2)$$

The line absorption cross section can be written as (e.g., Rybicki & Lightman 1979)

$$\sigma_{\nu}(V_{\parallel}) = f \frac{\pi e^2}{m_e c} \Phi[\nu - \nu_0(1 + V_{\parallel}/c)], \quad (3)$$

where f is the oscillator strength of a specific line transition, and Φ is the Voigt profile centered at $\nu_0(1 + V_{\parallel}/c)$ (with ν_0 the intrinsic line frequency). When thermal broadening dominates, we have $\Phi = 1/(\sqrt{\pi}\Delta\nu_T)$ at the line center, where $\Delta\nu_T$ is the thermal width. Since $\Delta\nu_T$ is much less than the bandwidth of transiting observations, the Voigt profile can be approximated by a delta function. Thus we have

$$\tau_{\nu} = f \frac{\pi e^2}{m_e c \nu_0} c \left(\frac{dN_i}{dV_{\parallel}} \right)_{V_{\parallel}=c(\nu-\nu_0)/\nu_0}, \quad (4)$$

where $(\pi e^2/m_e c \nu_0) = (10^{-16}/4)(\lambda_0/2800 \text{ \AA}) \text{ cm}^2$.

For WASP-12b, Fossati et al. (2010) found that the transit depths in the wavelength regions NUVA (2539–2580 \AA) and NUVC (2770–2811 \AA) are larger than the continuum depth by a factor of two at the 2.5σ level, implying the effective radii of order $2.69R_J$ and $2.66R_J$, respectively. The flux depletions in the 41 \AA window of NUVA and NUVC are produced by many absorption lines. If we require a single line (of a given atomic species i) to significantly deplete the flux (i.e., $\tau_{\nu} \gtrsim 1$) in the wavelength range $\Delta\lambda$ around its intrinsic wavelength λ_0 ,

then the column density of the gas with velocity around $V_{\parallel} = c\Delta\lambda/\lambda_0$ must satisfy

$$\begin{aligned} \left(\frac{dN_i}{d \ln V_{\parallel}} \right)_{V_{\parallel}=c\Delta\lambda/\lambda_0} &\gtrsim \frac{4 \times 10^{13}}{f} \left(\frac{2800 \text{ \AA}}{\lambda_0} \right) \left(\frac{\Delta\lambda/\lambda_0}{10^{-3}} \right) \text{ cm}^{-2} \\ &\simeq \frac{1.3 \times 10^{13}}{f} \left(\frac{2800 \text{ \AA}}{\lambda_0} \right) \left(\frac{V_{\parallel}}{100 \text{ km s}^{-1}} \right) \text{ cm}^{-2}. \end{aligned} \quad (5)$$

For example, for the Mg II 2800 \AA lines, $f = 0.93$, and if we take $\Delta\lambda = 1 \text{ \AA}$, we find $(dN_i/d \ln V_{\parallel}) \gtrsim 1.4 \times 10^{13} \text{ cm}^{-2}$ at $V_{\parallel} \simeq 108 \text{ km s}^{-1}$. For a characteristic length scale of $3R_p = 5.4R_J$ (see below), this corresponds to the gas density $dn_i/d \ln V_{\parallel} \gtrsim 400 \text{ cm}^{-3}$. Note that, since the thermal velocity of the Mg atom is $v_T = (kT/24m_H)^{1/2} = 1.9(T/10^4 \text{ K})^{1/2} \text{ km s}^{-1}$, such a large $\Delta\lambda/\lambda_0$ ($= 1/2800$, corresponding to $V_{\parallel} = c\Delta\lambda/\lambda_0 = 108 \text{ km s}^{-1}$) cannot be due to thermal broadening, but must arise from significant bulk motion of the absorbing gas along the line of sight. If we choose a smaller $\Delta\lambda$, (i.e., a single line covers a smaller range of wavelength in the absorption), the required column density is smaller, but then we would require a denser spectrum of absorption lines so that the whole 41 \AA wavelength regions of NUVA and NUVC are significantly absorbed.

Now consider the ingress/egress asymmetry in the transit of the NUVA band. Figure 2 of Fossati et al. (2010) shows that in optical continuum, the ingress starts at the orbital phase $\phi \simeq 0.945$, and the center of the transit is at $\phi = 1$. The phase difference of 0.055 corresponds to a transverse distance (projected on the plane of the sky) of $0.925R_{\star} + R_p \simeq 1.04R_{\star}$ (for the orbital inclination angle $i = 83.1^{\circ}$). In the NUVA band, the ingress starts at $\phi \simeq 0.925$ or earlier. The phase difference of 0.075 then corresponds to a transverse distance of $(0.075/0.055)(1.04R_{\star}) = 1.42R_{\star}$. This implies that the excess NUVA absorber during the ingress must extend a distance of at least $0.38R_{\star} \simeq 3.2R_p$ from the planetary surface.

The above constraints for the column density and size/location of the line absorber will be used to evaluate two possible models for the ingress/egress asymmetry in the following sections.

3. ROCHE LOBE OVERFLOW AND ACCRETION STREAM

3.1. Accretion Stream and Disk Formation

The gas dynamics of Roche lobe overflow in semidetached binaries was studied by Lubow & Shu (1975, 1976). Here we adapt their theory to mass transfer in close-in exoplanetary systems like WASP-12b (cf. Li et al. 2010).

Consider the atmosphere of the planet in quasi-hydrostatic equilibrium extending to its Roche lobe. As the gas flows through the L1 point, it transitions from subsonic to supersonic, with the sonic surface close to the L1 point. The size of the transonic nozzle at L1 is

$$\Delta R_L \sim c_s / \Omega_o, \quad (6)$$

where c_s is the sound speed and $\Omega_o = 2\pi/P$ is orbital frequency of the binary. The mass transfer rate is related to the gas density at L1 by

$$\dot{M} \sim \pi \rho_L c_s (\Delta R_L)^2. \quad (7)$$

The steady-state equation of motion of the gas in the rotating frame reads

$$\frac{d\mathbf{u}}{dt} = (\mathbf{u} \cdot \nabla)\mathbf{u} = -\nabla\Phi - 2\boldsymbol{\Omega} \times \mathbf{u} - \frac{\nabla P}{\rho}, \quad (8)$$

where $P = \rho c_s^2$ is the gas pressure, and Φ is the Roche potential:

$$\Phi = -\frac{GM_\star}{r_1} - \frac{GM_p}{r_2} - \frac{1}{2}\Omega_o^2 [(X+a-\mu a)^2 + Y^2]. \quad (9)$$

Here $\mu = M_p/(M_\star + M_p)$, $r_1 = r = \sqrt{X^2 + Y^2}$, $r_2 = \sqrt{(X+a)^2 + Y^2}$, and the coordinates (X, Y) are measured from the center of the star (see Fig. 1). The L1 point is determined from $\partial\Phi/\partial X = 0$ for $Y = 0$, giving the distance of L1 from the center of the planet:

$$x_L = a - |X_L| \simeq a \left(\frac{q}{3}\right)^{1/3} \left[1 - \frac{1}{3} \left(\frac{q}{3}\right)^{1/3}\right], \quad (10)$$

for $q = M_p/M_\star \ll 1$. The gas along a streamline conserves its Bernoulli integral (assuming constant c_s), $\mathcal{B} = \mathbf{u}^2/2 + \Phi + c_s^2 \ln \rho$. As the gas leaves L1 and accelerates toward the star, pressure becomes negligible at a distance larger than ΔR_L , and then the gas particle follows a ballistic trajectory. Due to the combined effects of Coriolis force and Roche potential force, the gas particle leaves the L1 region in a narrow stream (with width ΔR_L), along the direction given by the angle θ_s (the angle between streamline near L1 and the X-axis)

$$\cos 2\theta_s = -\frac{4}{3A} + \left(1 - \frac{8}{9A}\right)^{1/2}, \quad (11)$$

with $A = a^3 [\mu/r_1^3 + (1-\mu)/r_2^3]_{L1}$. Thus $\theta_s = 26.7^\circ$ for $q = 10^{-3}$ (and 28.4° for $q \rightarrow 0$). Figure 1 illustrates (in the case of $q = 10^{-3}$) the stream trajectory for several values of initial gas velocities comparable to the sound speed [$c_s/(a\Omega_o) = 0.02$, or $c_s \simeq 5 \text{ km s}^{-1}$ for the WASP-12 system.]

The crossings of streamlines lead to shock dissipation and disk formation. The stream collides with the disk at point D (see Fig. 1), whose position (and thus the outer radius of the disk r_d) is determined by the “no-slip” condition, i.e., the ϕ -component of the incident stream velocity equals the circular velocity at the same point, the latter being given by (in the corotating frame) $v_{\text{circ}} \simeq (GM/r)^{1/2} - r\Omega_o$ (for $q \ll 1$). Figure 2 shows the velocity of the accretion stream before it collides with the outer edge of the disk for the cases of $q = 0.001$ and 0.005 . We see that, for example, for $q = 0.001$, the stream impacts the disk at $|Y_d| = 0.24a$ and $r_d = 0.71a$, with the terminal velocity $u = 0.53a\Omega_o$ (and u_x reaches $0.38a\Omega_o$).

As the stream evolves from L1 to impact (point D), its width W undergoes relatively small variation, due to the combined effects of the finite sound speed (which tends to make the stream expand) and the enhanced gravity closer to the star (which tends to compress the stream). Thus, $W \simeq \Delta R_L$, and the cross-sectional area of the stream remains of order $\pi(\Delta R_L)^2$. The mean density of the stream therefore varies as

$$\rho_s \sim \rho_L \frac{c_s}{u}, \quad (12)$$

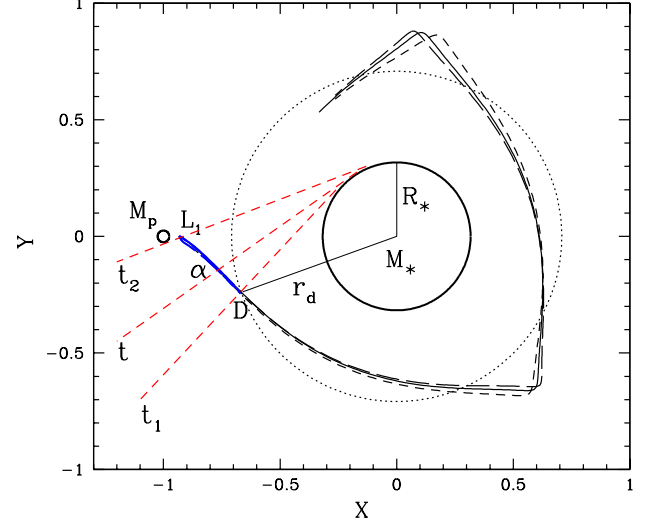


FIG. 1.— Stream trajectory and disk formation in the orbital plane for the case of planet-star mass ratio $q = M_p/M_\star = 10^{-3}$ (WASP-12b parameter). The planet is located at $(X, Y) = (-1, 0)$ (in units of a), and rotates counter-clockwise around the star. Three streamlines leaving L1 are shown, corresponding to the initial velocity (in units of the orbital velocity of the planet, $\sqrt{GM_\star/a} = 228 \text{ km s}^{-1}$) of $(u_x, u_y) = (0, 0)$ (solid line), $(0.02, 0)$ (dashed line) and $(0.02, -0.02)$ (long-dashed line). In the absence of a disk, matter would follow these stream trajectories. Self-collisions of the streams cause the formation of a disk. The disk outer radius is at $r_d = 0.71$. The stream strikes the disk at point D, beyond which the stream does not exist. The dashed straight line labeled t_1 indicates the line of sight when the star light is first blocked by the stream (the ingress of the “stream transit”), and the line labeled t_2 indicates the ingress of the “normal” planet transit. A general line of sight is labeled t , with the angle between the stream axis and the line of sight denoted by α .

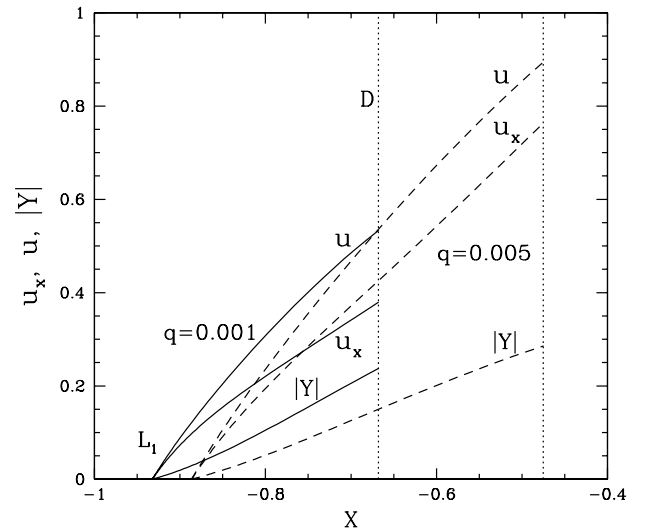


FIG. 2.— Stream trajectory and velocity for mass ratio $q = 0.001$ (solid lines) and 0.005 (dashed lines). The stream starts at L1 and terminates when it collides with the outer edge of the disk (the vertical dotted line labeled “D”). The star and planet are located at $(X, Y) = (0, 0)$ and $(-1, 0)$ (in units of a), respectively. The plotted quantities are u (stream velocity in the rotating frame, in units of the orbital velocity of the planet, $\Omega_o a = 228 \text{ km s}^{-1}$ for WASP 12-b), u_x (the X-component of the stream velocity) and $|Y|$ (the Y-position of the stream; see Fig. 1).

for the stream velocity $u \gtrsim c_s$.

Note that the “no-slip” condition likely only gives the minimum value of the outer disk radius (see Shu & Lubow 1981). In reality, tidal forces from the planet set the outer truncation of the disk. Numerical simulations of the planet-disk interaction in the Type II regime (in which the planet is sufficiently massive to open a gap in the gas disk; see Lin & Papaloizou 1993) typically find that the gap half width is about 0.2-0.3 a (e.g., Lubow & D’Angelo 2006; Armitage 2007). Thus we shall adopt the outer disk radius $r_d \simeq 0.7a$ in this paper.

The accretion disk formed from the stream has a steady-state surface density $\Sigma_d(r) \simeq \dot{M}/(3\pi\nu_d)$, where ν_d is the disk viscosity. Adopting the α -viscosity ansatz, $\nu_d = \alpha_d H_d c_{ds}$, where c_{ds} is the disk sound speed and $H_d = c_{ds}/\Omega_d(r)$ is the disk thickness, we find

$$\Sigma_d \simeq \frac{1}{3\alpha_d} \left(\frac{c_s}{c_{ds}} \right)^2 \left(\frac{\Omega_d}{\Omega_o} \right) \Sigma_L, \quad (13)$$

where $\Sigma_L \simeq \rho_L W$ is the gas column density at the L1 point. Obviously, for $\alpha_d \ll 1$, we expect $\Sigma_d \gg \Sigma_L$.

3.2. Application to the WASP-12 System

To estimate the gas density of the accretion stream in the WASP-12 system, we assume that the planet has an isothermal atmosphere with temperature $T \simeq 3000$ K (corresponding to a sound speed of $c_s \simeq 5$ km s $^{-1}$)⁵ and surface density $\rho(R_p) \sim 5 \times 10^{-8}$ g cm $^{-3}$ (see Li et al. 2010). Relative to the planet center, the Roche lobe extends to L1 at $x_L \simeq a(q/3)^{1/3} = 1.85 R_p$. Along the y -direction (in the orbital plane), it extends to $y_L = (2/3)x_L = 1.23 R_p$. Since the Roche potential along the planet’s y -axis (relative to the planet center) is simply $-Gm/y + \text{constant}$, one finds $\rho(y_L) \sim 3 \times 10^{-12}$ g cm $^{-3}$ (Li et al. 2010). Since the Roche lobe is an equipotential surface, this is also close to the density at L1. With the nozzle radius $\Delta R_L \sim 7.5 \times 10^4$ km $\simeq 0.6 R_p$ and a thermal outflow velocity c_s , we find that the mass transfer rate through L1 is $\dot{M} \sim 2.7 \times 10^{14}$ g s $^{-1} \simeq 3 \times 10^{-9} M_p$ yr $^{-1}$.

Note that Li et al. (2010) considered mass transfer driven by an energy source within the planet’s Roche lobe. Such an energy source may lie inside the planet, maintaining its inflated radius. The suggested energy source was tidal dissipation due to an assumed eccentricity of the orbit (see also Gu et al. 2003). It has since, however, become clear that the orbit of WASP-12b is highly circular ($e = 0.017 \pm_{0.011}^{0.015}$ from new radial-velocity monitoring; Husnoo et al. 2010), implying that such an eccentricity-driven tidal energy source is negligible. Li et al. obtained a much higher mass loss rate (about 25 times larger than our estimate) as they assumed that the matter flows from below the Roche lobe over the entire surface area of the Roche lobe. In our discussion below, we take a conservative approach and adopt our (smaller) value of \dot{M} given above, as we believe it sets the minimum value of the mass transfer rate.

The above discussion neglects the possible effect of the planet’s thermosphere, where photo-ionization

heats the gas temperature to $\sim 10^4$ K (e.g., Murray-Clay et al. 2009; Koskinen et al. 2010). Taking the photo-ionization cross section $\sigma_{\text{PI}} \simeq 6 \times 10^{-18} (\epsilon_0/13.6 \text{ eV})^{-3} \text{ cm}^2 \simeq 2 \times 10^{-18} \text{ cm}^2$ for photon energy $\epsilon_0 = 20$ eV, we find that the column density that UV photons can penetrate is $5 \times 10^{17} \text{ cm}^{-2}$. For $\rho_L \sim 3 \times 10^{-12} \text{ g cm}^{-3}$, this corresponds to a distance of 2.8 km, much less than ΔR_L . Thus, only the “skin” of the accretion stream will be affected by photo-ionization. This also shows that, the planet’s thermosphere, if any, lies outside the planet’s Roche lobe.

In principle, the Roche lobe, the accretion stream and the disk can all block the star light. Here we focus on the accretion stream since it is asymmetric relative to the line joining the star and the planet. To estimate the transiting property of the stream, we model it as a cylinder with length s_d and radius $W = \Delta R_L$. The result of Sect. 3.1 gives $s_d = 0.36a$ (for $X_d = -0.668$ and $Y_d = -0.238$; see Fig. 2). Thus the area of the stream as projected in the plane of the sky is $s_d W \sin \alpha \simeq 6R_p^2 \sin \alpha$, where α is the angle between the line of sight and the symmetry axis of the cylinder. Note that α varies during the transit (see Fig. 1). Clearly, if the stream is opaque to the radiation, it would lead to significant blockage of the star light, comparable to that produced by the planet itself.

To evaluate the column density of the stream, we need to know how the density varies along the stream. As discussed in Sect. 3.1, in the supersonic region, the density decreases as u^{-1} as the stream velocity u increases. Figure 2 shows that u increases approximately as a linear function of s , the distance from L1 along the stream. Thus we adopt $u(s) \simeq c_s/F(s)$, with $F(s) = 1$ for $0 < s < W$ and $F(s) = W/s$ for $W \leq s < s_d$. This gives $\rho \simeq \rho_L F(s)$. The hydrogen column density in the stream along the line of sight is then $N_H(s) \simeq (\rho/m_H)(W/\sin \alpha) \sim 10^{22} F(s)/\sin \alpha \text{ cm}^{-2}$. With $V_{\parallel} = c_s(s/W) \cos \alpha$ for $s > W$, we find

$$N_H \sim 10^{21} \left(\frac{100 \text{ km s}^{-1}}{V_{\parallel} \tan \alpha} \right) \text{ cm}^{-2} \quad (14)$$

for $V_{\parallel} \gtrsim 5 \cos \alpha \text{ km s}^{-1}$ (where we have used $c_s = 5 \text{ km s}^{-1}$). Thus, as long as the metal abundance satisfies $N_i/N_H \gtrsim 10^{-8} f^{-1} \tan \alpha (V_{\parallel}/100 \text{ km s}^{-1})^2$, the stream column density would be larger than that required by Eq. (5). For example, the solar abundance of Mg relative to H is 3×10^{-5} , and the Mg II 2800 Å lines (with $f = 0.93$) may then produce significant absorption of the star light. For Scandium, the solar abundance is about 10^{-9} , thus stronger lines with $f \gtrsim 10$ or a super solar abundance would be needed to produce significant line absorption (note that WASP-12a is supersolar by about 0.3; Hebb et al. 2009). We note that if the gas velocity (at a given s) is uniform within the cross-section of the stream, then the difference in the gas velocity along a given line-of-sight is $\Delta V_{\parallel} \sim c_s \cos^2 \alpha / \sin \alpha$. This is too small to produce significant reduction in the observed flux. However, it is possible that the 3D gas velocity structure in the stream is more complicated (e.g., due to the turbulence developed at the surface of the stream via Kelvin-Helmholtz instability) and a larger velocity difference along the line-of-sight could be produced.

⁵ The equilibrium temperature of the planet ranges from 2500 K to 3000 K, depending on the albedo and the efficiency of heat redistribution in the planetary atmosphere.

The collision between the accretion stream and the disk produces a hot spot, which may lead to time-dependent obscuration of the star light and possibly early ingress (C. Baruteau & D. Lin, 2010, private communication). As shown above [see Eq. (13)], the accretion disk formed from the stream has a significant surface density, and can cause obscuration of the star light. Obviously, a perfectly symmetric disk would only give time-independent obscuration. However, disk asymmetry (e.g., produced by the hot spot) may cause an apparent earlier ingress of the planet transit. Numerical simulations will be needed to assess these possibilities.

Our discussion so far has focused on the accretion stream due to mass transfer through the inner Lagrangian point L1. In general, an outward-spiraling stream may also form due to mass loss through the L2 Lagrangian point (S. Lubow, private communication)⁶. The L2 point is located at a distance $x_{L2} \simeq a(q/3)^{1/3} \left[1 + (1/3)(q/3)^{1/3} \right]$ from the center of the planet, farther away from the host star than the planet. The (Roche) potential difference between L1 and L2 is

$$\Phi_{L2} - \Phi_{L1} = \frac{2}{3} \frac{GM_p}{a}. \quad (15)$$

If we assume that the Roche lobe overflow through L1 does not affect the density of the outer L2 Roche lobe, we can estimate the density at L2 as $\rho_{L2} \simeq \rho_{L1} \exp(-2GM_p/3ac_s^2)$. For the WASP-12b parameters, we find $\rho_{L2}/\rho_{L1} \simeq 0.2$ for $c_s = 5 \text{ km s}^{-1}$ (see also Gu et al. 2003). In reality, ρ_{L2}/ρ_{L1} will be somewhat smaller than the above estimate, and a lower night-side temperature of the planet will also reduce ρ_{L2} . We conclude that the spiral stream from L2 is less important than the accretion stream. Numerical simulations of the two streams would be useful to accurately evaluate their relative effects on the planet transit.

4. MAGNETOPAUSE

The star WASP-12a resembles the Sun in many aspects, and we will parametrize its wind property using the observed solar wind parameters. The fiducial solar wind mass flux is $\dot{M}_w = 3 \times 10^{-14} M_\odot \text{ yr}^{-1}$. At 1 AU, the typical solar wind speed is of order 450 km s^{-1} (but can change on various timescales from 200 km s^{-1} to 1000 km s^{-1}), and the electron density, temperature and magnetic field in wind are $\sim 7 \text{ cm}^{-3}$, $1.4 \times 10^5 \text{ K}$, and $7 \times 10^{-5} \text{ G}$, respectively (e.g., Hundhausen 1995). Thus, the solar wind at 1 AU has a plasma β (the thermal pressure divided by the magnetic pressure) of order unity, and the fast magnetosonic Mach number is about 6 (Russell & Walker 1995).

To obtain the stellar wind property at the distance appropriate to WASP-12b ($a = 0.023 \text{ AU}$) requires detailed wind models, which we will not attempt here. But it is very likely that at such a small distance, the stellar wind is subsonic and sub-Alfvénic, and the fast magnetosonic Mach number is less than unity (e.g., Mestel & Spruit 1987; Cranmer 1998). For example, using the simplest (isothermal) Parker wind solution (for $M_\star = 1.35 M_\odot$),

⁶ G. Trammell, P. Arras and Z. Li (2010, to be submitted) have also recently considered this issue.

we find that if the wind speed at 1 AU is 500 km s^{-1} , then the sonic point is at 0.032 AU , and the wind velocity and Mach number at 0.023 AU are 90 km s^{-1} and 0.66 , respectively. (For a wind speed of 600 km s^{-1} at 1 AU, the corresponding numbers become 0.024 AU , 148 km s^{-1} and 0.94 .) The solar wind temperature actually increases with decreasing distance, and this will make the Mach number at 0.023 AU even smaller. The plasma β in the wind may reach below 0.1 at such a distance, with the wind magnetic field dominated by the radial component.

Given that at 0.023 AU , the stellar wind has a fast magnetosonic Mach number less than unity, we do not expect bow shock to form when the wind interacts with the planet's magnetic field. Instead, near the planet, the wind will be "gradually" stopped at the magnetopause. Importantly, since the orbital velocity of the planet, $v_{\text{orb}} = 228 \text{ km s}^{-1}$, is comparable to the wind velocity at 0.023 AU , $v_w \sim 100 \text{ km s}^{-1}$, the head of the magnetopause is shifted eastward with respect to the substellar point by an angle $\tan^{-1}(v_{\text{orb}}/v_w)$ ($= 66^\circ$ for $v_w = 100 \text{ km s}^{-1}$).

In general, the location of the magnetopause is determined by balancing the momentum flux ($P + \rho v_\perp^2 + B_\parallel^2/8\pi$) across the contact surface, where P is the gas pressure, v_\perp is the gas velocity perpendicular to the surface, and B_\parallel is the magnetic field parallel to the surface (e.g., Shu 1992). The standoff distance r_m (measured from the center of the planet) at the head of the magnetopause is obtained by

$$\rho_w(v_w^2 + v_{\text{orb}}^2) + P_w + \frac{B_w^2}{8\pi} = P_p + \frac{B_p^2}{8\pi} \left(\frac{R_p}{r_m} \right)^6, \quad (16)$$

where P_p is the gas pressure of the planetary magnetosphere, and we have assumed that the planet has a dipolar magnetic field with the equatorial strength B_p . In the absence of a detailed wind model, we parameterize Eq. (16) by

$$f_w \rho_w v_w^2 = f_p \frac{B_p^2}{8\pi} \left(\frac{R_p}{r_m} \right)^6. \quad (17)$$

We estimate $f_w \simeq 1 + v_{\text{orb}}^2/v_w^2 + \mathcal{M}^{-2} \sim 10$ (for $v_w \sim 100 \text{ km s}^{-1}$ and the fast magnetosonic Mach number $\mathcal{M} \sim 0.5$), and $f_p \sim 1$. With $\dot{M}_w = 4\pi a^2 \rho_w v_w$, we then have

$$\frac{r_m}{R_p} = 2.6 f_p^{1/6} (f_w v_{w1} M_{w1})^{-1/6} B_{p1}^{1/3}, \quad (18)$$

where $f_{w1} \equiv f_w/10$, $v_{w1} \equiv v_w/(100 \text{ km s}^{-1})$, $M_{w1} \equiv \dot{M}_w/(3 \times 10^{-14} M_\odot \text{ yr}^{-1})$ and $B_{p1} = B_p/(1 \text{ G})$. We see that the main uncertainty in our estimate of r_m is the magnetic field strength of the planet. For example, if $B_p \sim 5 \text{ G}$, the magnetopause may extend to $4.4 R_p$. Note that r_m is similar to the required extension of the absorbing gas to produce the asymmetric ingress/egress in WASP-12b (see Sect. 2). This motivates us to consider the possibility that the gas (from the stellar wind) around r_m may absorb the star light.

The number density of H in the stellar wind (before

any compression) at $a = 0.023$ AU is given by

$$n_H^{(0)} = \frac{\dot{M}_w}{4\pi a^2 v_w m_H} = 7.7 \times 10^4 \dot{M}_{w1} v_{w1}^{-1} \text{ cm}^{-3}. \quad (19)$$

As the stellar wind gas is deflected at the magnetopause, it may undergo some compression (of order unity) and move around the field lines at the velocity comparable to $v_w \sim 100 \text{ km s}^{-1}$. Whether this gas can provide enough line absorption to explain the observation depends on the physical states of the gas. Given the low gas density in Eq. (19), we consider the most optimistic scenario: If the gas around r_m is able to cool to 10^4 K (the equilibrium temperature between photo-ionization heating and collisional cooling) from 10^6 K (the original stellar wind temperature) while maintaining pressure equilibrium, it may be undergo compression by a factor of 100. Thus the characteristic hydrogen column density is

$$N_H \sim 100 n_H^{(0)} r_m \sim 3 \times 10^{17} f_p^{1/6} (f_{w1}^{-1} v_{w1}^{-7} M_{w1}^5)^{1/6} B_{p1}^{1/3} \text{ cm}^{-2}. \quad (20)$$

Comparing this with Eq. (5), we see that, under this optimistic condition, sufficient metal column density may be attained when $n_i/n_H \gtrsim 5 \times 10^{-5}$, which is of the same order as the stellar abundance of Magnesium⁷. Obviously, a larger \dot{M}_w would result in a higher gas column density.

It thus seems that the compressed gas at the magnetopause might just be able to cause enhanced absorption before ingress. The interaction of the stellar wind with planetary magnetospheres is, however, much more complex than discussed above (e.g., Kivelson & Russell 1995). Our estimate in Eq. (20) suggests that such interaction may produce observable effects. Further study on this subject in the context of hot Jupiters is worthwhile (cf. Preusse et al. 2007; Ekenbäck et al. 2010).

5. DISCUSSION

Motivated by the recent near-UV spectral observations of the WASP-12 planetary system (Fossati et al. 2010), which showed an earlier ingress of the planet's transit

compared to the optical continuum, we have studied two possible explanations for the ingress/egress asymmetry. The first involves mass transfer through Roche lobe overflow, which results in an elongated accretion stream in which gas flows from the L1 Lagrangian point toward the star. Our analysis of the geometric and velocity structure of the stream shows that it may indeed provide asymmetric obscuration of the star light during the planet transit. In addition, it is also possible that an asymmetry in the accretion disk, caused by the impact of the accretion stream, produces an apparent earlier ingress. Another possibility involves the magnetopause separating the stellar wind and the planetary magnetosphere. Because of the planet's orbital motion, the head magnetopause lies eastward relative to the substellar point. We suggest that line absorption by the gas around the magnetopause may also explain the asymmetric ingress/egress behavior, although more theoretical works are needed to understand the property of the absorbing gas around the magnetopause.

The two possibilities studied in this paper may be distinguished by the fact that in the accretion stream, the gas falls away from the observers, producing redshifted absorption, while the flow around the magnetosphere tends to move toward the observer, thus producing blueshifted absorption.

Finally, we note the observed behaviors reported by Fossati et al are only marginally significant (at most 3σ effects). Thus, more observations will be useful. Nevertheless, the physical processes discussed in this paper are quite general and therefore may be applicable in other close-in exoplanetary systems.

We thank the participants of the morning coffee of the KITP Exoplanets program (2010.1-2010.5) for lively discussions. D.L. especially thanks Phil Arras, Doug Lin and Steve Lubow for useful discussion during the final phase of our work, and P. Arras for his comments on an earlier draft of our paper. C.H. thanks Luca Fossati for discussion of early-ingress observations. Part of this work was performed while the authors were in residence at KITP, funded by the NSF Grant PHY05-51164.

REFERENCES

- Armitage, P.J. 2007, arXiv:astro-ph/0701485
 Bochsler, P., & Geiss, J. 1989, in *Solar System Plasma*, eds. J.H. Waite et al. (Washington DC: AGU), pp. 133-141
 Campo, Ch. et al. 2010, *ApJ*, submitted (arXiv:1003.2763)
 Cranmer, S.R. 1998, *ApJ*, 508, 925
 Ekenbäck, A., et al. 2010, *ApJ*, 709, 670
 Fossati, L., et al. 2010, *ApJ*, 714, L222
 Garcia Munoz, A. 2007, *Planet. Space Sci.*, 55, 1426
 Gu, P.-G., Lin, D.N.C., & Bodenheimer, P.H. 2003, *ApJ*, 588, 509
 Hebb, L. et al. 2009, *ApJ*, 693, 1920-1928
 Hundhausen, A.J. 1995, in *Introduction to Space Physics*, eds. M.G. Kivelson & C.T. Russell (Cambridge Univ. Press), p. 91
 Husnoo, N., et al. 2010, *MNRAS*, submitted (arXiv:1004.1809)
 Kivelson, M.G., & Russell, C.T. 1995, *Introduction to Space Physics* (Cambridge Univ. Press)
 Koskinen, T.T., Yelle, R.V., Pavvas, P., & Lewis, N.K. 2010, arXiv:1004.1396
 Li, S.-L., Miller, N., Lin, D. & Fortney, J. 2010, *Nature*, 463, 1054
 Lin, D.N.C., & Papaloizou, J.C.B. 1993, in *Protostars and Planets III*, ed. E.H. Levy & M.S. Matthews (Tucson: Univ. Arizona Press), 749
 Lubow, S.H., & D'Angelo, G. 2006, *ApJ*, 641, 526
 Lubow, S.H., & Shu, F.H. 1975, *ApJ*, 198, 383
 Lubow, S.H., & Shu, F.H. 1976, *ApJ*, 207, L53
 Mestel, L., & Spruit, H.C. 1987, *MNRAS*, 226, 57
 Murray-Clay, R.A., Chiang, E.I., & Murray, N. 2009, *ApJ*, 693, 23
 Preusse, S., et al. 2007, *Planetary & Space Sciences*, 55, 589
 Russell, C.T., & Walker, R.J. 1995, in *Introduction to Space Physics*, eds. M.G. Kivelson & C.T. Russell (Cambridge Univ. Press), p.503
 Rybicki, G.B., & Lightman, A.P. 1979, *Radiative Processes in Astrophysics* (Wiley-VCH)
 Schneider, E.M., et al. 2007, *ApJ*, 671, L57-L60
 Shu, F.H. 1992, *Gas Dynamics* (University Science Books)
 Shu, F.H., & Lubow, S.H. 1981, *ARAA*, 19, 277
 Tian, F., et al. 2005, *ApJ*, 621, 1049
 Yelle, R.V. 2004, *Icarus*, 170, 167

⁷ What is of interest here is the metal abundance of the stellar wind, which is unknown. In the case of the Sun, it is known that

the solar wind metal abundance can be larger than the abundance at the solar atmosphere (e.g., Bochsler & Geiss 1989).